

## POLARIZATION, JETS, AND THE DISTRIBUTION OF CIRCUMSTELLAR DUST AROUND T TAURI STARS AND OTHER YOUNG INFRARED SOURCES

PIERRE BASTIEN

Observatoire du Mont Mégantic and Département de Physique, Université de Montréal

Received 1985 February 19; accepted 1986 November 18

### ABSTRACT

Available linear polarization data and information about jets and bipolar outflows observed near T Tauri stars and other young infrared objects are used in conjunction with polarization models to discuss the distribution of circumstellar dust grains around these stars. Two general cases are investigated: (1) axially symmetric distributions of spherical grains and (2) nonspherical grains aligned preferentially in some direction. It is shown that if case 1 is assumed, then one can distinguish between two families of models: (a) where the polarizing dust is distributed in an oblate configuration as in a circumstellar disk around the star and (b) where the dust lies in a prolate configuration as in two oppositely directed jets. If, on the other hand, the polarization is due to linear dichroism instead of scattering (case 2), then asymmetric grains are aligned preferentially perpendicular to the plane of the disk; if the alignment is by a magnetic field, the field is predominantly in the plane of the disk, contrary to some models proposed recently to explain the jets. The distribution of the linear polarization is considered, and also the information on position angles of the polarization and of the jets. Other possible explanations, e.g., with polarization reversals, are discussed and the constraints derived. The data show that both cases considered occur in T Tauri stars, and that in case 1 a prolate configuration for the polarizing dust in the optical is to be preferred.

*Subject headings:* polarization — stars: circumstellar shells — stars: pre-main-sequence — stars: winds

### I. INTRODUCTION

Evidence for a stellar wind in T Tauri stars is not new (Kuhi 1964). However, it has recently been found that at some distance from the star the matter propagates not isotropically but rather in two opposite directions. Evidence for this has come from radio observations of bipolar outflow (e.g., Snell, Loren, and Plambeck 1980 for L1551 IRS 5; see the reviews by Snell 1983 and Lada 1985) and from optical jets observed at  $H\alpha$  and at a few other emission lines near some T Tauri stars (Craine, Boeshaar, and Byard 1981; Mundt and Fried 1983; see the reviews by Mundt 1985 and Strom 1986 for lists of references).

Variable linear polarization was found in T Tauri stars by Vardanian (1964) and Serkowski (1969). The mechanism responsible for the polarization was later identified (Bastien and Landstreet 1979) as being due mostly to scattering of radiation from the stars and their surrounding gas-emitting regions in external circumstellar dust envelopes. More recently, surveys of linear polarization in T Tauri stars have become available (Bastien 1982, 1985). They include all known bright ( $V$  or  $m_{pg} \leq 13$  mag) T Tauri stars in both hemispheres.

Various alignments with the direction of linear polarization have been studied recently. Kobayashi *et al.* (1978), Dyck and Lonsdale (1979), and Heckert and Zeilik (1981) (see also § IV and Table 4) studied the relationship between the polarization of young infrared (IR) sources and the interstellar (IS) polarization in their neighborhood. For a sample of 52 sources, they found that 58% showed IR position angles differing by less than  $30^\circ$  from the general IS position angles as determined from optical polarimetry of surrounding field stars, and 38% showed differences between these two position angles of more than  $45^\circ$ . Their interpretation was that most IR sources are polarized by nonspherical grains aligned by a magnetic field parallel to the IS magnetic field, while the polarization in the other sources was presumed to be due to scattering.

Another alignment was found to exist between the direction of CO molecular outflows and the IS magnetic field (Cohen, Rowland, and Blair 1984), and also between the direction of optical jet sources and the IS magnetic field (Strom *et al.* 1986; see § IV and Table 4). By noting that there is no preferential alignment of bipolar outflows with the Galactic plane (Bally and Lada 1983), Cohen, Rowland, and Blair (1984) conclude that the correlation is indeed with the magnetic field, and not, for example, with the direction of Galactic rotation. Their interpretation is that the IS magnetic field constrains collapse along its field lines to form disks perpendicular to the field. Then the field and the gas density gradient would have directed the flow along the field, as proposed by Königl (1982).

Comparison of the position angles of the jets or the CO molecular outflows and of the linear polarization (optical and IR) shows that they are nearly perpendicular to each other within the observational errors (e.g., Mundt and Fried 1983; Nagata, Sato, and Kobayashi 1983; Hodapp 1984; § IV and Table 3). The favored explanation is that of scattering particles mostly in the lobes of bipolar sources, as proposed by Elsässer and Staude (1978).

It is both interesting and puzzling here to note that this is not what one observes in extragalactic jets. The optical  $E$ -vector lies *parallel*, and the radio  $E$ -vector normal, to the VLBI structural axis in a sample of sources with mostly “core-jet” VLBI morphology (e.g., Rusk and Seaquist 1985). Here we will consider only stellar sources and jets.

Since both the linear polarization data and the jets provide constraints on the geometrical distribution of the matter surrounding these stars, they should be considered together. The relations between the jets and the linear polarization are discussed further in this paper.

Models to explain the polarization in young stellar objects (YSOs) can be divided into two groups: dust-scattering models

and models with aligned grains. Analytic models for producing polarization by scattering in optically thin envelopes around single stars have been presented by Brown and McLean (1977, hereafter BM) for electrons, and more recently by Simmons (1982) for spherical dust grains. These analytic models are examined critically in § IIa in the context of YSOs. Non-spherical dust grains can be aligned by various mechanisms. The models with magnetic field proposed recently to explain the jets in YSOs could be efficient at aligning grains. Those models are examined in § IIb. The observed and true polarization frequency distributions are considered in § III under the assumption of the dust-scattering models. The position angles of jets and of linear polarization are compared with predictions of both scattering and aligned grain models in § IV.

## II. MODELS FOR PRODUCING CIRCUMSTELLAR POLARIZATION IN YOUNG SOURCES

### a) Scattering Models with Axial Symmetry

#### i) Electron Scattering

In the case of Thomson scattering in an optically thin axially symmetric circumstellar envelope surrounding a point source star, BM have shown that the residual polarization which one observes is given by the simple formula

$$P_R \approx 2\bar{\tau}(1 - 3\gamma) \sin^2 i,$$

where  $i$  is the usual inclination of the symmetry axis to the line of sight,  $\gamma$  is a shape factor related to the flatness of the envelope, and  $\bar{\tau}$  is an average optical depth. (Note the factor of 2 missing in BM's eq. [23]). The shape factor is defined by the ratio of two moment integrals of the axially symmetric but otherwise arbitrary density distribution. The value of the shape factor is particularly important, since it determines the sign of the polarization. Here a negative polarization means that the position angle of the electric vector is perpendicular to the axis of symmetry.

It is instructive to consider four models:

*Model 1.*—A disk, where the matter is concentrated in the equatorial plane, so that  $\gamma = 0$ , and  $P_R \approx 2\bar{\tau} \sin^2 i$ .

*Model 2.*—The matter is distributed in two oppositely directed jets, so that  $\gamma = 1$ , and  $P_R \approx -4\bar{\tau} \sin^2 i$ .

*Model 3.*—We consider an annular cylinder of uniform density contained between inner radius  $R_1$ , outer radius  $R_2$ , and height  $H$  on either side of a plane of symmetry containing the star. With the variables  $h = H/R_1$ , and  $\rho = R_2/R_1$ , the shape factor is given by (BM)

$$\gamma = \left\{ 2 + \frac{h \log [(\rho^2 + h^2)/(1 + h^2)]}{\rho \arctan(h/\rho) - \arctan h} \right\}^{-1}.$$

In the limit  $h \rightarrow 0$ ,  $\gamma \rightarrow 0$  and  $P_R \rightarrow 2\bar{\tau} \sin^2 i$ , which is the same result as in case 1 above, whereas for an infinitely long cylinder,  $h \rightarrow \infty$ ,  $\gamma \rightarrow \frac{1}{2}$  and  $P_R \rightarrow -\bar{\tau} \sin^2 i$ , which is to be compared to case 2.

*Model 4.*—Finally, consider a cylindrical sector of uniform density contained between two lines of constant polar angle  $\theta$  making an angle of  $2\varphi_0$ . In this case  $\gamma = \frac{1}{3} \sin^2 \varphi_0$ , and  $P_R = 2\bar{\tau} \cos^2 \varphi_0 \sin^2 i$ ; the limits  $\varphi_0 \rightarrow 0^\circ$ , which yields  $\gamma \rightarrow 0$ ,  $P_R \rightarrow 2\bar{\tau} \sin^2 i$ , and  $\varphi_0 \rightarrow 90^\circ$ , which gives  $\gamma \rightarrow \frac{1}{3}$ ,  $P_R \rightarrow 0$ , correspond to a plane distribution (e.g., the same as case 1), and a sphere, respectively.

We note that only factors of 2 or 4 in the polarization, and the direction of polarization, distinguish cases of elongated geometry (2 or 3 with  $h \rightarrow \infty$ ) and of "flat" geometry (1, 4, or 3

with  $h \rightarrow 0$ ). While more realistic, models 3 and 4 give essentially the same results as models 1 and 2.

#### ii) Dust Scattering

Since the polarization in T Tauri stars is due mostly to dust grains (Bastien and Landstreet 1979), we now consider models involving dust. For spherically symmetric dust particles in an axially symmetric but otherwise arbitrary density distribution, the residual polarization is given by

$$P = 3 \sin^2 i |\bar{F}_{22}(k)N_2|,$$

in the first-order approximation (Simmons 1982). For Thomson and Rayleigh scattering, this approximation is exact. In the case of Mie scattering, this approximation is valid when  $x = ka = (2\pi/\lambda)a < 2.0$ , where  $a$  is the grain radius. For a typical size  $a = 0.1 \mu\text{m}$ , this corresponds to  $\lambda > 0.3 \mu\text{m}$ .  $N_2$  is in general complex and determined entirely by the density distribution.  $\bar{F}_{22}$  is real and depends on the scattering phase function; it determines the wavelength dependence of the polarization. The position angle in this approximation is given by

$$\pm \frac{1}{2} \arg N_2^*,$$

where the asterisk denotes the complex conjugate. The sign depends on  $\bar{F}_{22}$ . Thus, as  $\lambda$  varies, the position angle will remain constant, except for a possible swing by  $\pi/2$  when  $\bar{F}_{22}$  changes sign. Otherwise the position angle is determined by the density distribution of scatterers alone (Simmons 1982).

*Case 1.*—For a plane disk using a density distribution given by  $n(r, \theta, \phi) = \delta(\theta - \pi/2)n'(r)$ , then

$$N_l = \frac{2l+1}{2} P_l(0) \int_0^\infty n'(r) dr = \frac{2l+1}{2} P_l(0)N',$$

which is zero for  $l$  odd, because of the symmetry. Here,  $P_l$  are the Legendre polynomials. In this case we have, in the first approximation,

$$P \approx \frac{1}{4}(N' \sin^2 i) \bar{F}_{22}.$$

The position angle here is perpendicular to the disk, except for a possible change by  $\pi/2$  when  $\bar{F}_{22}$  changes sign.

*Case 2.*—For a polar line with  $n(r, \theta, \phi) = n''(r)\delta(|\cos \theta| - 1)$ , one finds

$$N_l = \frac{2l+1}{2} \int_0^\infty n''(r) dr = \frac{2l+1}{2} N''.$$

The polarization in the first approximation is then

$$P \approx \frac{1}{2}(N'' \sin^2 i) \bar{F}_{22}.$$

The position angle is perpendicular to the polar line, except again possibly when  $\bar{F}_{22}$  changes sign.

*Case 3.*—The problem of the annular cylinder was solved by Simmons (1982) for different values of the ratio  $A = R_1/2H$  with the inner radius  $R_2$  set to zero. Again, the limits are expected to be similar, in the first-order approximation, to the problem of electron scattering.

*Case 4.*—For the cylindrical sector considered above, the density distribution is given by

$$n(r, \theta, \phi) = \begin{cases} n_d, & \frac{\pi}{2} - \varphi_0 < \theta < \frac{\pi}{2} + \varphi_0, \\ 0, & \text{otherwise.} \end{cases}$$

Then

$$N_2 = \frac{5}{2} n_d R \sin \varphi_0 \cos^2 \varphi_0$$

and

$$P = \frac{15}{2} n_d R \bar{F}_{22},$$

where  $R$  is the radius of the sphere containing the cylindrical sector. The position angle is along the axis of symmetry, except for possible changes in sign of  $\bar{F}_{22}$ .

For Thomson scattering, one can show (Simmons 1982) that  $\bar{F}_{22} = \sigma_T/20$ , where  $\sigma_T$  is the usual Thomson scattering cross section. By substitution of this value for  $\bar{F}_{22}$  in the four results above for spherical dust grains, it is easy to show that they reduce to the equivalent results for electrons which were considered first by BM. (Note again a factor of 2 missing in their eq. [37].)

The similar  $\sin^2 i$  dependence in the first-order approximation to the polarization for all axisymmetric density distributions, and in the particular cases considered above, prevents us from finding out which case is the prevalent one in T Tauri stars, assuming that scattering models are appropriate, by making use of the observed and true polarization (frequency) distributions (see § III). There remains the difference in sign, or difference in position angle, which distinguishes cases with oblate or prolate geometries. This comparison is made in § IV, but first we consider models in which the grains are aligned.

#### b) Models with Aligned Grains

An alternative explanation to the models of scattering by spherical grains in asymmetric stellar envelopes discussed above is given by models in which the polarization is due to nonspherical, aligned dust grains in a circumstellar disk around the star. Two models involving magnetic fields have been proposed recently to explain the observed bipolar outflows. These are the centrifugally driven wind model of Pudritz and Norman (1983), Pudritz (1985), and the so-called sweeping magnetic twist model of Uchida and Shibata (1984*a, b*, 1985*a, b*). According to these models, the magnetic field in the disk is mostly perpendicular to the disk. Therefore, nonspherical grains should be aligned predominantly perpendicular to the field, and the light is predicted to be polarized by dichroic absorption perpendicularly to the disk.

One can also consider a purely poloidal magnetic field, which approaches the plane of symmetry at a polar angle  $\theta$ , and which leaves it at the angle  $\pi - \theta$ . In other words, the disk bisects the angle made by the incoming and outgoing field lines. We consider now grains aligned by such a field, and find the direction of the polarization that one would measure through a diaphragm centered on the object. The polarization is found to be parallel to the disk for  $45^\circ < \theta < 135^\circ$ , and perpendicular to it otherwise. Therefore, from stellar polarimetry alone (as opposed to imaging polarimetry), one cannot distinguish between the field configuration just discussed with  $\theta < 45^\circ$  and a field strictly perpendicular to the disk, or similarly between the case  $45^\circ < \theta < 135^\circ$  and a purely toroidal field.

### III. OBSERVED AND TRUE FREQUENCY DISTRIBUTIONS OF THE POLARIZATION

The frequency distribution of the polarization data available in the literature for T Tauri stars and a few more massive (Ae/Be) young stars are considered in this section, under the

assumption that scattering models are the appropriate ones for all (or almost all) these stars.

#### a) Observed Frequency Distributions

All the polarization data given in the two surveys by Bastien (1982, 1985) can be used for a statistical study of the shape of the envelopes around T Tauri stars. A similar study has been carried out for Be stars (McLean and Brown 1978, hereafter MB). Since for dust scattering in the first-order approximation, the intrinsic polarization for the four cases considered above (§ II*a*) has the same form as for Thomson scattering (i.e., higher order terms in  $\sin i$  do not appear), such an analysis is justified for T Tauri stars.

If one assumes that the symmetry axes of T Tauri stars are randomly oriented, then the probability distribution of the inclination angle  $i$  is simply  $\sin i$ . Other distributions for  $i$  have been considered by Bernacca (1970). Then the true  $f(p)$  and observed  $\psi(P_R)$  polarization distributions are related by an Abel equation (MB) for which a formal solution exists. However, this is an ill-conditioned equation, so that stringent conditions must be set on the observed distribution to obtain a poorly determined true distribution (for more details see the discussion in MB). The practical method for obtaining some information about the true distribution is to find out how its moments relate to the moments of the observed distribution, a method used by Chandrasekhar and Münch (1950) for the distribution of rotational velocities. The moments, the mean square deviation, and skewness of the distribution for  $p$  are related to  $P_R$  by

$$\begin{aligned} \bar{p} &= \frac{3}{2} \bar{P}_R, & \overline{p^2} &= \frac{15}{8} \overline{P_R^2}, & \overline{p^3} &= \frac{35}{16} \overline{P_R^3}, \\ \overline{(p - \bar{p})^2} &= \frac{15}{8} \overline{P_R^2} - \frac{9}{4} \bar{P}_R^2, \\ \overline{(p - \bar{p})^3} &= \frac{35}{16} \overline{P_R^3} - \frac{135}{16} \bar{P}_R \overline{P_R^2} + \frac{27}{4} \bar{P}_R^3. \end{aligned}$$

Note that an error in MB in the equation corresponding to the last equation above has been corrected.

The sample contains all T Tauri stars brighter than 13th magnitude, and a few fainter ones. It is the same sample used by Bastien (1985) for his correlation searches between polarization and other properties of T Tauri stars. Two bandpasses have been used, with central wavelengths and full widths at half-maximum 5895 (700), and 7543 (875) Å. A histogram of the observed polarizations is presented in Figure 1. The results are given in Table 1. The numbers give the fractional polarization, not the polarization in percent. The mean, the root mean square deviation, and the skewness calculated from the formulae above are also given. The mean value of the true polarization distributions at 5900 and 7540 Å are both relatively large. For comparison, MB found 0.7% for a sample of 67 Be stars. These two distributions are rather broad, since the rms deviations are nearly equal to the mean value. They are also strongly skewed, the skewness being about twice the rms deviation. Although the true distribution cannot be uniquely specified from these values, some general properties may be deduced (§ III*c*).

#### b) Contributions to the Observed Polarization

Before discussing the general properties of the distributions, it is necessary to consider the various possible contributions to the observed polarization. In principle, there are four components to the observed polarization: (i) IS, (ii) a component due to intracluster dust, as in the Orion Nebula (cf. Breger 1977, 1978), (iii) intrinsic polarization arising in a circumstellar

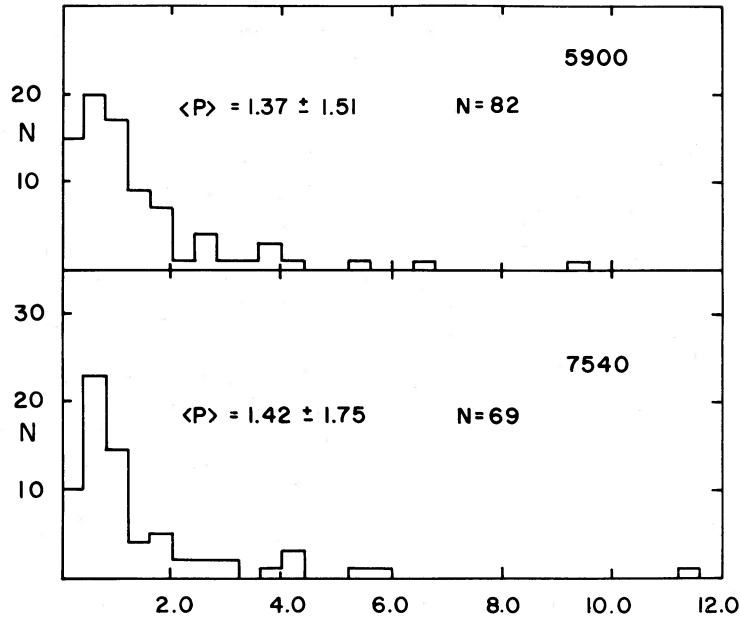


FIG. 1.—Histogram of the linear polarization data in two bandpasses centered on the wavelengths indicated. The average polarization, standard deviation, and number of stars in each case are indicated.

environment, and (iv) polarization arising in stellar photospheres. There is strong evidence that component (iii) above is the dominant one in most T Tauri stars: (a) Polarization variability occurs in at least 60% (maybe up to 85%) of T Tauri stars with sufficient data (Bastien 1985; Ménard 1986; Ménard and Bastien 1987). The variations may indicate that the dust is confined close to a plane or to a relatively narrow solid angle. (b) The wavelength dependences of the polarization observed for more than 20 T Tauri stars display a large variety of curves, which in all but a few cases look quite different from the expected shape for IS or intracluster polarization. (c) The large polarizations observed in some T Tauri stars are too large to be due to components (i) or (ii) above. (d) There is no difference in polarization across emission or absorption features with respect to the nearby continuum, which excludes component (iv). Even though component (iii) dominates, one should try to evaluate the importance of components (i) and (ii). This has been done for a few stars in Bastien (1985). However, this is not easily done and requires more data than are available for most stars. Since the true distribution of the observed polarizations cannot be specified uniquely anyway, only the effects that small

to moderate IS and/or intracluster polarizations have on the general properties of the distributions will be discussed.

#### c) Discussion of the Polarization Distributions

Two general properties of the polarization distributions can be deduced. The effects of IS or intracluster dust polarization are discussed below. First, there is no maximum observed polarization which constrains the models. For Be stars, a cutoff was found at 2%, and this fact was interpreted by MB as meaning that polarizations larger than 2% are difficult to obtain because of the presence of direct unpolarized light from the star, and probably also because extremely oblate envelopes do not occur. For T Tauri stars, this does not happen. Large polarizations are found, and contribute to the skewness of the distributions. One way to obtain such large polarizations is to absorb a good fraction of the direct unpolarized light by, for example, an equatorial disk. This appears to be the case in HL Tau, where we are apparently looking at the disk edge-on (Cohen 1983). If this explanation is the correct one, then large polarizations are not expected to be common, since the viewing angle is not always favorable (recall the  $\sin^2 i$

TABLE 1  
MOMENTS OF OBSERVED AND TRUE DISTRIBUTION FUNCTIONS OF LINEAR POLARIZATION

STATISTIC	$\lambda = 5900, N = 82$		$\lambda = 7540, N = 69$	
	$P_R = p \sin^2 i$	$p$	$P_R = p \sin^2 i$	$p$
$\bar{X}$ .....	$1.370 \times 10^{-2}$	$2.055 \times 10^{-2}$	$1.420 \times 10^{-2}$	$2.130 \times 10^{-2}$
$\overline{X^2}$ .....	$4.148 \times 10^{-4}$	$7.778 \times 10^{-4}$	$5.068 \times 10^{-4}$	$9.503 \times 10^{-4}$
$\overline{X^3}$ .....	$3.510 \times 10^{-5}$	$7.678 \times 10^{-5}$	$5.252 \times 10^{-5}$	$1.149 \times 10^{-4}$
$[(X - \bar{X})^2]^{1/2}$ .....	$1.507 \times 10^{-2}$	$1.885 \times 10^{-2}$	$1.747 \times 10^{-2}$	$2.228 \times 10^{-2}$
$[(X - \bar{X})^3]^{1/3}$ .....	$2.852 \times 10^{-2}$	$3.588 \times 10^{-2}$	$3.322 \times 10^{-2}$	$4.189 \times 10^{-2}$

dependence), and also, even if the angle is appropriate, the dust density may be low in some cases. For example, older T Tauri stars could have a lower dust density in their immediate surroundings because of their past activity which repelled most of the circumstellar material.

The behavior of the distributions at low polarization values is more difficult to explain. Although there are some T Tauri stars with a small intrinsic polarization which have been reasonably well studied (e.g., SU Aur), most stars with a small polarization have not been observed often enough to allow a discussion of their polarization variability and wavelength dependence. Some of the small polarizations may be of interstellar (IS) or intracluster origin. Bearing in mind this fact, one might interpret the decrease in the number of stars with small polarization as indicating that, for most T Tauri stars, the dust distribution as seen from the Earth is not spherically symmetric. It is clear from the above discussions that this is the case for the few highly polarized T Tauri stars. However, the point here is that this would be true for the majority of T Tauri stars. For, if the dust distribution were spherically symmetric for most of them, then one would obtain a distribution peaking sharply at  $P = 0\%$ . Such a distribution is observed in Be stars (MB), where one expects circumstellar envelopes more nearly spherically symmetric and/or of low electron density to be more readily produced than highly flattened envelopes. A nonspherical dust distribution around T Tauri stars is expected if these stars are born in molecular disks (e.g., Pudritz 1986).

Let us now examine how these two properties are modified by the presence of IS polarization. The first point about the large polarizations and the skewness of the distributions is clearly not an artifact due to IS or intracluster polarization. The other point, related to the low-polarization stars, may be affected to some extent by IS polarization. A small IS polarization affecting all T Tauri stars in a given cloud cannot be ruled out, and is in fact to be expected. Hence, the conclusion mentioned above that the distribution of circumstellar dust around most T Tauri stars is not spherically symmetric but instead strongly prolate, for example, can for the time being be considered only as plausible.

#### IV. THE MODELS AND THEIR QUALITATIVE COMPARISON WITH OBSERVATIONS

##### a) Scattering Models with Axial Symmetry

Since the polarization frequency distributions do not allow discrimination between the scattering models considered above, we now consider the information available on position angles. At first sight, one would say that the polarization vector, perpendicular to the scattering plane, should be along the axis in cases 1 (the disk), 3 (the annular cylinder, when  $h \rightarrow 0$ ), and 4 (the cylindrical sector), and perpendicular to the axis in the other cases. And since most of the jets which have been observed so far are perpendicular to the polarization vector, one is led to conclude that the polarizing dust lies in two (or only one in some cases) oppositely directed jets. A similar model has been proposed by Elsässer and Staude (1978) to explain the BN source.

However, a change by  $90^\circ$  in position angle of the linear polarization has been observed in the infrared for T Tau at  $\sim 1.6 \mu\text{m}$  and probably also for SU Aur at  $\sim 1.2 \mu\text{m}$  (Hough *et al.* 1981). Similar polarization reversals have been observed in red variable stars, e.g., VY CMa and R Aql (Forbes 1971; Dyck, Forbes, and Shawl 1971; McCall and Hough 1980).

Daniel (1980) found that for a given refractive index, the polarization reversal occurs always at the same value of  $x = 2\pi a/\lambda$ , for all envelope geometries, optical depths, and direction of observation. Polarization reversals are found to occur mostly for dielectrics, i.e., particles with a small imaginary (absorptive) part in their refractive index, and not for other, more conductive grains. Values of  $x_0$ , the value of  $x$  at which the polarization reversal occurs, have been plotted by Simmons (1982) as a function of the real part of the refractive index using the first-order approximation. The values may be used for envelopes with small optical depths, but for others the values of  $x_0$  depend on higher order terms.

The value of  $x_0$  for silicate grains is 1.89 (Daniel 1980; Simmons 1982), increasing slightly for "dirty" silicates. Therefore, the reversal will occur at  $\lambda_0 = 3.32a$ , or somewhat less than this for "dirty" silicates. For T Tau this gives  $a = 0.5 \mu\text{m}$ , and for SU Aur,  $a = 0.4 \mu\text{m}$ . On the other hand, the wavelength dependence of the polarization in T Tau is rather flat and requires iron grains of diameters  $0.3\text{--}0.4 \mu\text{m}$ , or graphite grains of  $0.3$  to  $>0.6 \mu\text{m}$  diameter (Bastien 1981), to be fitted. Although the sizes are comparable, iron and graphite grains do not show the change by  $\pi/2$  in position angle which is characteristic of dielectrics. However, we should note that the interpretation in the case of T Tau may be more complicated, since it has an infrared companion at  $\sim 0.6$  to the south (Cohen, Biegging, and Schwartz 1982; de Veigt 1982; Simon *et al.* 1983; Hanson, Jones, and Lin 1983). A third companion at  $0.3$  to the north has been found recently by Nisenson *et al.* (1985) in the optical. In order to have a disk model (case 1, case 3 with  $h \rightarrow 0$ , or case 4) with a polarization parallel to the disk in the visible, the grain radius must be no larger than  $0.10 \mu\text{m}$  for pure silicate grains or  $0.12 \mu\text{m}$  for "dirty" silicates (refractive index =  $1.65 - 0.1j$ ). This cannot be ruled out definitely, but is less likely than case 2 or case 3 with  $h \rightarrow \infty$ , in which the polarizing grains are located in the jets and the polarization is normally perpendicular to the jets. The oblate models are even less likely given the fact that the constraint on grain composition and grain radius would have to apply to all jet sources with a perpendicular polarization.

One can also explain the polarization reversals with a model involving two optically thin lobes and a thick disk. The polarization at small wavelengths (e.g., in the visible), is caused by dust scattering in the optically thin lobes. At longer wavelengths, the optical depth in the lobes becomes negligible, and the polarization from scattering off dust grains in the disk dominates, thus producing a change by  $90^\circ$  in the position angle. When the two mechanisms for polarization reversals, i.e., based on dielectrics and based on geometry, are considered together, then the wavelength at which the  $90^\circ$  switch occurs is moved to longer wavelengths (Daniel 1982). The mechanism based on different optical depths is more likely to apply in general to T Tauri stars and YSOs because it does not require severe constraints on grain size and grain composition.

##### b) Position Angles of Jets and Polarization

In order to compare the models with the observations, a compilation of jet sources is presented in Table 2. Only jets or outflows for which the central source (or probable central source) has been found and its linear polarization measured are included in this table. The columns give, respectively, (1) the name of the central star and the associated Herbig-Haro (HH) object, (2) the position angle of the jet,  $\vartheta_{\text{jet}}$ , as observed in the optical, and (3)  $\vartheta_{\text{jet}}$  as observed in the CO molecular line,

TABLE 2  
COLLIMATED OUTFLOW SOURCES WITH MEASURED LINEAR POLARIZATION

STAR/JET (1)	$\vartheta_{\text{jet}}$		$\vartheta_*$ (4)	$\vartheta_{\text{IS}}$ (5)	$ \Delta - 90^\circ $ (6)	TYPE (7)	REFERENCES (8)	NOTES (9)
	Optical (2)	Radio (3)						
GL 490 .....	...	$13^\circ \pm 10^\circ$	$115^\circ \pm 1^\circ$	$116^\circ$	$12^\circ$	I	1-3	
SVS 13/HH 7-11 .....	$142^\circ \pm 5^\circ$	...	$65 \pm 3$	$147 \pm 9$	13	I	1, 4, 5	
DG Tau .....	$226 \pm 2$	...	$136 \pm 1$	45	0	T	6-9	1
Haro 6-10 .....	65	...	$111 \pm 11$	59	44	T:	4, 9	1
L1551 IRS 5 .....	$243 \pm 2$	...	$161 \pm 1$	76	8	F	1, 6, 10-12	1
HH 30 IR/HH 30 .....	$29 \pm 2$	...	$93 \pm 10$	76	26	T?	4, 6, 13	1
HL Tau .....	$37 \pm 3$	...	$147 \pm 1$	76	20	T	6-8, 11	1
Haro 6-13 .....	245	...	140	59	15	T:	4, 9	1
V380 Ori .....	56, 149	...	$90 \pm 2$	146	56, 31	H	4, 7, 14	1
NGC 2071 IR .....	...	50	$142 \pm 13$	$115 \pm 6$	2	I	15-18	
LkH $\alpha$ 208 .....	0	...	$2 \pm 5$	$171 \pm 2$	88	H	14, 18-20	1
GL 961/GGD 18 .....	...	$150 \pm 20$	$92 \pm 5$	170	32	W:H	4, 21-23	?1
R Mon/HH 39 .....	5, 190 $\pm$ 5	...	$96 \pm 3$	173	1, 4	H	4, 14, 20, 24-26	1
Serpens nebula (S68) .....	$110 \pm 10$	...	$65 \pm 10$	$64 \pm 4$	45	?	18, 27	1
S CrA .....	80	...	$156 \pm 3$	110	14	T	4, 8	?1
R CrA .....	$130 \pm 5, 315 \pm 5$	...	$9 \pm 5$	110	59	H	4, 14, 28, 29	?1
T CrA .....	$133 \pm 5$	...	$18 \pm 5$	110	25	H	14, 28	1
AS 353 A/HH 32 .....	107	...	$144 \pm 3$	$15 \pm 20$	53	T	7, 18, 30, 31	1
Parsamyan 21 .....	155	...	$75 \pm 4$	$18 \pm 18$	10	?	18, 32	1
1548C27 .....	54	...	$7 \pm 2$	$20 \pm 2$	43	T:	18, 31, 33, 34	
GL 2591 .....	...	30, 260	172	$40 \pm 31$	2, 52	I	1, 23, 34, 35	
LkH $\alpha$ 234 .....	$55 \pm 10$	$35 \pm 15$	28, 45v	$48 \pm 7$	60-90	H	14, 18, 20, 29	1
LkH $\alpha$ 233 .....	50, 90	...	147	$87 \pm 7$	7	H	14, 18, 36	1

NOTES.—(1) See list below.

NOTES ON INDIVIDUAL SOURCES

*DG Tau* (= IRAS 04240 + 2559) (Rucinski 1985).—Strom *et al.* 1986 give  $\vartheta_{\text{jet}} = 228^\circ$ . *DG Tau* has no significant circular polarization in the red (Nadeau and Bastien 1986). The linear polarization is variable (Bastien 1985).

*Haro 6-10* (= IRAS 04263 + 2426).—Within L1524. A possible jet, but spectroscopic data are required for confirmation. Strom *et al.* 1986 list it as a "wider, collimated flow."

*L1551 IRS 5*. (= IRAS 04287 + 1801).—This object may be an FU Orionis star (Mundt *et al.* 1985).

*HH 30 IR*. Strom *et al.* 1986 give  $\vartheta_{\text{jet}} = 40^\circ$ .

*HL Tau* (= IRAS 04287 + 1807).—Probably includes contributions from HL and XZ Tau. The jet may come from another source, or it is bent. In the latter case, the  $\vartheta_{\text{jet}}$  given here is the value far from the star, not as the jet leaves it.

*Haro 6-13* (= IRAS 04292 + 2422).—Strom *et al.* 1986 think that a jet may be traced out by three knots seen at H $\alpha$  about 4' from Haro 6-13, and which define a line passing through the star. Confirmation is required.

*V380 Ori*.—The polarization of the star could be variable (Vrba, Schmidt, and Hintzen 1979); however, contamination by the reflection nebula is significant in the blue.

*LkH $\alpha$  208*.—The  $\vartheta_*$  given is for the "I" band; values for other filters can be found in Vrba, Schmidt, and Hintzen 1979, where the polarization of this star is classified as possibly variable.

*GL 961*.—This object is in fact a double star with a separation of 5".8 at a position angle of 254° (Lenzen, Hodapp, and Reddmann 1984; Castelaz *et al.* 1985). The  $\vartheta_*$  given here (from Garrison and Anderson 1978) includes both components. Castelaz *et al.* 1985 give  $\vartheta_* = 97^\circ \pm 3^\circ$  (961E) and  $\vartheta_* = 75^\circ \pm 3^\circ$  (961W). Sato *et al.* 1985 obtained  $\vartheta_* = 81^\circ \pm 2^\circ$  in the *K* band for both components together. This yields a range of (37°, 15°) for  $|\Delta - 90^\circ|$ . See also the discussion in Strom *et al.* 1986. According to Castelaz *et al.* 1985, GL 961W is a young Ae/Be star (type H), and GL 961E would be a B2-B5 ZAMS star.

*R Mon/HH 39*.—The polarization and its position angle are variable (Vrba, Schmidt, and Hintzen 1979).

*Serpens nebula*.—The pre-main-sequence nature of the central source has not yet been established.

*S CrA*.—A nebulosity, possibly an HH object, was found by Strom *et al.* 1986 at P.A.  $\approx 80^\circ$  from S CrA. It is not clear that a jet is associated with this star.

*R CrA*.—A heavily obscured star, IRS 7, with *K-L* = 4.6 mag, was found between R and T CrA by Taylor and Storey 1984. Its role in the region is not clear at present. The values of  $\vartheta_{\text{jet}}$  given here are for two small-scale jets close to R CrA. A larger scale flow involving HH 99, HH 100, and HH 101 may also be present at  $\vartheta_{\text{jet}} = 40^\circ$  (Hartigan and Lada 1985; Strom *et al.* 1986).

*T CrA*.— $\vartheta_*$  is  $\sim 0^\circ$  ("B" to "R"), but is  $133^\circ \pm 5^\circ$  at "I" in Vrba, Schmidt, and Hintzen 1979.

*AS 353 A/HH 33*.—The companion is at 6" in 175° and is about 2 mag fainter (Herbig and Rao 1972). The polarization of this star does not seem to vary (Bastien 1982).

*Parsamyan 21*.—The pre-main-sequence nature of this star still has to be shown. Neckel and Staude 1984 propose an A5 V central star obscured by  $A_V = 4$  mag at  $d = 0.4$  kpc to fit the available *UBVJHK* photometry. The IS polarization determined from 22 stars within a 6° radius from Parsamyan 21 gives a different result when the points are weighted linearly with distance from the star ( $18^\circ \pm 18^\circ$ ), or when no weight is used: P.A. =  $47^\circ \pm 23^\circ$ . This shows that the alignment changes on a scale smaller than 6°.

*LkH $\alpha$  234*.—The polarization and its P.A. vary (Vrba, Schmidt, and Hintzen 1979). The interpretation of the region containing LkH $\alpha$  234 is far from trivial, since there may be two or even three outflow sources (Hartigan and Lada 1985). LkH $\alpha$  234 shows a monopolar red lobe in CO (Lada 1985).

*LkH $\alpha$  233*.—The optical flow directions are somewhat ambiguous: there are elongations in the isophote map in directions of 50°, 90°, 230°, and 270°. The polarization vector map near the central source shows clearly a disk structure in the direction of 140°, perpendicular to the brightness features at 50° and 230°. The  $\vartheta_*$  in Vrba, Schmidt, and Hintzen 1979 is between 154° ("B") and 150° ("I").

REFERENCES.—(1) Hodapp 1984; (2) Kobayashi *et al.* 1978; (3) Lada and Harvey 1981; (4) Strom *et al.* 1986; (5) Turnshek, Turnshek, and Craine 1980; (6) Mundt and Fried 1983; (7) Bastien 1982; (8) Bastien 1985; (9) Moneti *et al.* 1984; (10) Nagata, Sato, and Kobayashi 1983; (11) Vrba, Strom, and Strom 1976; (12) Draper, Warren-Smith, and Scarrott 1985c; (13) Cohen and Schmidt 1981; (14) Vrba, Schmidt, and Hintzen 1979; (15) Heckert and Zeilik 1981; (16) Bally 1982; (17) Heckert and Zeilik 1984; (18) this paper. (19) Shirt, Warren-Smith, and Scarrott 1983; (20) Garrison and Anderson 1978; (21) Lenzen, Hodapp, and Reddmann 1984; (22) Lada and Gautier 1982; (23) Dyck and Lonsdale 1979; (24) Walsh and Malin 1985; (25) Aspin, McLean, and Coyne 1985; (26) Gething *et al.* 1982; (27) King, Scarrott, and Taylor 1983; (28) Ward-Thompson *et al.* 1985; (29) Hartigan and Lada 1985; (30) Mundt, Stocke, and Stockman 1983; (31) Mundt 1985; (32) Draper, Warren-Smith, and Scarrott 1985a; (33) Craine, Boeshaar, and Byard 1981; (34) Mundt *et al.* 1984; (35) Sato *et al.* 1985; (36) Aspin, McLean, and McCaughrean 1985.

TABLE 3  
DISTRIBUTION OF THE POSITION ANGLE DIFFERENCE  $|\Delta - 90^\circ|$

$ \Delta - 90^\circ $ Range	Number of Sources	Names
0°–15° .....	8 + 3	GL 490, SVS 13/HH 7–11, DG Tau, L1551 IRS 5, Haro 6–13, NGC 2071 IR, R Mon, (S CrA), (Parsamyan 21), (GL 2591), LkH $\alpha$ 233
16–30 .....	3	HH 30 IR/HH 30, HL Tau, T CrA
31–45 .....	3 + 1	Haro 6–10, GL 961/GGD 18, (Serpens nebula), 1548C27
46–60 .....	3	V380 Ori, R CrA, AS 353A
61–75 .....	1	LkH $\alpha$ 234
76–90 .....	1	LkH $\alpha$ 208

(4) the position angle of the polarization of the central source,  $\vartheta_*$ , (5) the IS polarization position angle,  $\vartheta_{IS}$ , (6)  $|\Delta - 90^\circ|$ , where  $\Delta = \vartheta_{jet} - \vartheta_*$  (the optical jet position angle was preferred, when available), (7) the type of the central source (defined below), and (8) reference numbers to the literature. A “1” appears in column (9) if there are comments on an individual source at the end of the table. If there is a doubt about the relation of the jet to the central source, or to which component, in case of a double source, the jet belongs, a question mark appears in the last column. All the data have been compiled from the literature, except when no  $\vartheta_{IS}$  could be found. In that case, the IS polarization was computed from a compilation of polarization catalogs following the prescription given in Bastien (1985). Those values of  $\vartheta_{IS}$  have been computed with a linear weight inversely proportional to the angular distance from the stars of interest.

There are 23 entries, a few of them dubious for reasons given in the notes. The sample contains eight T Tauri or probable T Tauri stars (indicated by a T appearing in col. [7] of Table 2), eight young Ae/Be or probable Ae/Be stars (H), one probable FU Orionis object (F) (L1551 IRS 5; Mundt *et al.* 1985), four IR sources (I), and two objects with unknown status (?). A colon (or question mark) in column (7) means that the type of object is somewhat (or more) uncertain. The W in this column for GL 961/GGD 18 indicates that the identification applies to the western component, GL 961W, of the pair. At least as many known jet sources have been excluded in this list for various reasons, the main one being that there is no polarization available for the central source. Others were excluded because the central source is not detected in the visual or IR, e.g., Cep A/GGD 37 (Lenzen, Hodapp, and Solf 1984; Hartigan and Lada 1985), RNO 138/NGC 7129 (Draper, Warren-Smith, and Scarrott 1985b), VLA 1/HH 1, 2, 3). For S140, the flow, if bipolar, is viewed nearly pole-on (Lada 1985; Joyce and Simon 1986). Also, T Tau has a high-velocity outflow westward toward an HH object (Bührke, Brugel, and Mundt 1986), but it is not clear from which one of the three components it originates, and the polarimetry (visual and near-IR) includes all of them. One source, Haro 6-5B, has a measured polarization: it is “polarized at a level of 6% with position angle also perpendicular to the jet” (Scarrott *et al.* 1986). However, these authors do not give the value of the position angle or its error, so that it cannot be included in Table 2.

Table 3 displays the distribution of the position angle difference  $|\Delta - 90^\circ|$ . One sees that for 11 (48%) or perhaps 14 (61%) sources out of 23, the directions of the outflow and of the polarization are within  $30^\circ$  of being perpendicular to each other. Sources with a dubious status are given in parentheses and counted separately. Similarly, the position angles of the

jets and the IS polarization tend to be aligned parallel to each other (Table 4). However, the intrinsic and IS polarizations tend to be perpendicular to each other, as expected from the two previous relations, but only marginally (Table 4). From an examination of the individual sources, one finds four of them which have a jet parallel to the IS polarization and perpendicular to the intrinsic polarization to within  $15^\circ$ : SVS 13/HH 7–11, L1551 IRS 5, Haro 6–13, and R Mon. If one relaxes the constraint to  $30^\circ$ , T CrA also fits in. On the other hand, the jet, the IS, and the intrinsic polarizations are all parallel to each other to within  $15^\circ$  for LkH $\alpha$  208 or to within  $30^\circ$  for LkH $\alpha$  234. For these two stars, the wavelength dependence of the stellar polarization is quite different from the IS polarization curve (see Vrba, Schmidt, and Hintzen 1979). The polarization of LkH $\alpha$  208 is probably due to scattering by dust in a small disk close to the star. This star, and possibly also LkH $\alpha$  234 (but see the notes in Table 2), is an exception to the general picture presented above of an optically thick disk and optically thin lobes, although the difference might be only one of optical depth and/or grain density.

### c) Models with Aligned Grains

Probably the best evidence in favor of aligned-grain models are the polarization maps of bipolar outflow sources such as R and T CrA (Ward-Thompson *et al.* 1985), L1551 IRS 5 (Draper, Warren-Smith, and Scarrott 1985c), LkH $\alpha$  233 (Aspin, McLean, and McCaughrean 1985) the Serpens nebula (King, Scarrott, and Taylor 1983), Parsamyan 21 (Draper, Warren-Smith, and Scarrott 1985a), R Mon and NGC 2261 (Gething *et al.* 1982; Aspin, McLean, and Coyne 1985). These observations show that the polarization is parallel to the disk, contrary to the prediction of the models with aligned grains (§ IIb). Probably one should change these models to have a predominantly toroidal field in the disk, even though the field may leave the

TABLE 4  
DISTRIBUTION OF POSITION ANGLE DIFFERENCES

Range	$ \vartheta_{jet} - \vartheta_{IS} \pm n\pi $	$ \vartheta_* - \vartheta_{IS} \pm n\pi $
0°–15° .....	9 $\frac{1}{2}$ <sup>a</sup>	5
16–30 .....	4	2
31–45 .....	4	0
46–60 .....	2	7
61–75 .....	1	1
76–90 .....	2 $\frac{1}{2}$ <sup>a</sup>	7

<sup>a</sup> V380 Ori has two “luminous protuberances” in directions almost perpendicular to each other (see Table 2 and Strom *et al.* 1986). Each one was counted as  $\frac{1}{2}$  for the present purpose.

disk at an angle approaching  $90^\circ$ . However, even though the case for grain alignment in the above sources is good, the outflow characteristics of some of them (the Serpens nebula, Parsamyan 21) still has to be made. There are other bipolar sources with no evidence for aligned grains, e.g., LkH $\alpha$  208 (Shirt, Warren-Smith, and Scarrott 1983), OH 0739-14 (Heckert and Zeilik 1983), and RNO 138 near NGC 7129 (Draper, Warren-Smith, and Scarrott 1985b).

The polarization maps show that the grains in the disks of some sources are aligned. It would seem natural to assume that the light coming from the star is also polarized in the same manner, i.e., that the linear polarization observations in  $5''$ - $15''$  diaphragms centered on T Tauri stars are due to aligned grains. In such a model, the temporal variations in the intrinsic position angle of the polarization can be explained by small changes in grain alignment, which could be due, for example, to fluctuations in the flow in the region where the dust lies.

In the centrifugally driven wind model, the density in the disk increases as one approaches the accretion region from outside, and, when the density increases above  $10^{11} \text{ cm}^{-3}$ , the ionization fraction becomes very low, and the charges on grains are not sufficient to prevent the magnetic field from leaving. Therefore, in that model, there is no magnetic field in regions close to the star where the density is above  $10^{11} \text{ cm}^{-3}$  (Pudritz 1986; R. Pudritz 1985 private communication). On the other hand, in dust-scattering models, the grains closest to the star are expected to contribute most to the polarization, as can be seen from, e.g., the "one-particle" dust cloud model in Bastien and Landstreet (1979). If the closest grains are in the high-density region with no (or little) magnetic field, then polarization by scattering could be important when the star is observed, even though the grains farther away are aligned.

Another possibility is that grains are aligned by another mechanism. Wolstencroft and Simon (1975) interpreted their observations of variable circular polarization in the FU Orionis star V1057 Cyg (with signal-to-noise ratio of about 3) in terms of changes in the alignment of dust grains in a disk seen pole-on. Dolginov and Mytrophanov (1978) pursued the analysis further by considering alignment by magnetic fields, gas outflow, and radiation pressure. For V1057 Cyg they favor alignment of prolate and oblate grains by the combined effect of gas outflow and the magnetic field which is frozen into the plasma. However,  $V \sin i = 45 \text{ km s}^{-1}$  for this star (Hartmann and Kenyon 1985). For more details on the interpretation see Nadeau and Bastien (1986).

Nadeau and Bastien (1986) have recently detected circular polarization in the continuum in three out of five T Tauri stars. After discarding an IS origin, they are led in some stars to multiple scattering and in some others to grain alignment.

#### V. DISCUSSION

There are strong and weak arguments in favor of or against both types of models: dust scattering and aligned grains. These are summarized in Table 5.

One limitation of the scattering models discussed here for both electrons (BM) and dust (Simmons 1982 and the specific models computed in § II) is that they all assume single scattering only, so that one is restricted to small optical depths ( $\tau \lesssim 0.3$ ). However, one would expect the matter in the jets to be mostly optically thin, while the confining disk around the star is most likely optically thick. This seems required in order to absorb enough direct unpolarized stellar light and yield a high polarization. Multiple scattering in homogeneous axisym-

TABLE 5  
FACTORS CONSTRAINING THE POLARIZATION MODELS

Dust Scattering	Aligned Grains
Factors Favoring Models	
Correlation between polarization and brightness variations <sup>a</sup>	Maps with aligned polarization vectors
Wavelength dependence of linear polarization	Temporal variations of position angle <sup>b</sup>
Temporal variations of position angle <sup>c</sup>	Circular polarization
Circular polarization <sup>d</sup>	
Factors against Models	
Maps with aligned polarization vectors	Correlation between polarization and brightness variations <sup>a</sup>
	Wavelength dependence of linear polarization
	Polarization reversals
	Large ( $\Delta P > 1\%$ and/or $\Delta\theta_* > 30^\circ$ ) and rapid ( $\Delta t < 1-3$ days) polarization variations <sup>e</sup>

<sup>a</sup> At least one star has shown such a correlation, RY Lup, during 12 consecutive nights. The best model appears to be that of a spotted star in rotation illuminating an asymmetric dust cloud in which the star is embedded (Bastien *et al.* 1987).

<sup>b</sup> The variations are explained by changes in grain alignment for these models.

<sup>c</sup> These variations in position angle ( $\theta_*$ ) are explained by density fluctuations in the flow or changes in the illumination of the grains for the dust-scattering models.

<sup>d</sup> Circular polarization in the dust-scattering models implies multiple scattering and large optical depth. Single scattering of unpolarized light cannot produce circular polarization.

<sup>e</sup> The alignment mechanisms probably cannot adjust rapidly enough to explain these variations.

metric ellipsoids cannot produce polarizations greater than 12% (Daniel 1980), and therefore an inhomogeneous density distribution as in a bipolar nebula is required to reproduce the large polarizations observed in the infrared for some of the sources given in Table 2. Models incorporating multiple scattering (Ménard and Bastien 1987) should therefore improve on the single-scattering models considered here.

Nadeau and Bastien (1986) found that in some stars multiple scattering in an asymmetric envelope explains best the linear and circular polarization data, and in other stars, dichroic extinction by aligned grains seems required. In view of all the arguments given above in favor of and against both types of models, it thus appears that none of them can explain all the observations, and both are required. This agrees with the conclusion reached by Heckert and Zeilik (1981) from consideration of the alignment of intrinsic and IS polarizations for infrared sources. Comparison of these infrared polarization data with scattering models led Heckert and Zeilik (1985) to conclude that scattering in a bipolar geometry seems able to explain the data for most sources. Alignment needs to be invoked in only a few sources.

However, the general alignment of the infrared polarization (e.g., Dyck and Lonsdale 1979; Heckert and Zeilik 1981), and

also the optical polarization (e.g., Moneti *et al.* 1984) with the IS polarization, still needs an explanation. The reader is reminded here that the infrared and optical polarization in these YSOs is mostly intrinsic, i.e., circumstellar, for the reasons given in § IIIb. The following scenario seems plausible. The magnetic field plays a significant role on a large scale and constrains clouds to collapse along the field lines to form sheets. Then the sheets fragment into disks, a central object forms in the center of those disks, and then bipolar outflows are set up. The polarization is then due to dust scattering usually in optically thin lobes (in the optical), or to aligned grains in a predominantly toroidal field configuration ( $\theta$  must satisfy at least  $45^\circ < \theta < 135^\circ$ ). Therefore, one must be very careful not to conclude that the polarization in YSOs is due to grain alignment by a magnetic field *because* the direction of polarization in infrared sources is aligned with the IS magnetic field. The magnetic field may have played a role indeed, but only indirectly.

#### VI. SUMMARY AND CONCLUSIONS

Available linear polarization data and information on jets in T Tauri stars and other pre-main-sequence objects have been used to discuss the distribution of circumstellar material around them. Two polarizing mechanisms have been considered: dust scattering and dichroic absorption by aligned grains. Both mechanisms are required in order to explain all the available data, some stars requiring scattering, the others

requiring aligned grains. The arguments for and against each mechanism are summarized in Table 5.

Two families of scattering models have been considered: oblate geometries, e.g., a disk, and elongated ones, e.g., two oppositely directed jets. The distribution of the linear polarization does not allow one to distinguish between the two groups, although the large polarizations observed in some cases could be explained by absorption of some of the direct stellar unpolarized light by a circumstellar disk. Comparison of the position angles of the polarization and jets or bipolar outflows would indicate that the polarizing dust lies most probably in the jets, although there are exceptions. Polarization reversal has been observed in T Tauri stars; however, it is not likely that it occurs in all sources with bipolar outflow. The most likely explanation of the polarization reversal is in terms of differing optical depths in the lobes and in the disk.

When aligned, nonspherical grains are required, if the alignment is by a magnetic field, then the field must be predominantly in the plane of the disk, i.e. a toroidal field, or the field lines must leave the plane at a small angle to the plane ( $< 45^\circ$ ).

I thank R. E. Pudritz for very fruitful and stimulating discussions, and an anonymous referee for comments and suggestions which led to improvements in the paper. I also thank R. Mundt for making available a list of position angles of optical jets. This research was supported by the National Research Council of Canada.

#### REFERENCES

- Aspin, C., McLean, I. S., and Coyne, G. V. 1985, *Astr. Ap.*, **149**, 158.  
 Aspin, C., McLean, I. S., and McCaughrean, M. J. 1985, *Astr. Ap.*, **144**, 220.  
 Bally, J. 1982, *Ap. J.*, **261**, 558.  
 Bally, J., and Lada, C. J. 1983, *Ap. J.*, **265**, 824.  
 Bastien, P. 1981, *Astr. Ap.*, **94**, 294.  
 ———, 1982, *Astr. Ap. Suppl.*, **48**, 153; **48**, 513.  
 ———, 1985, *Ap. J. Suppl.*, **59**, 277.  
 Bastien, P., and Landstreet, J. D. 1979, *Ap. J. (Letters)*, **229**, L137.  
 Bastien, P., Le Van Suu, A., Bouvier, J., Bertout, C., Ménard, F., Boivin, L. 1987, in preparation.  
 Bernacca, P. L., 1970, in *Stellar Rotation*, ed. A. Slettebak (Dordrecht: Reidel), p. 227.  
 Breger, M. 1977, *Ap. J.*, **215**, 119.  
 ———, 1978, *Ap. J.*, **223**, 180.  
 Brown, J. C., and McLean, I. S. 1977, *Astr. Ap.*, **57**, 141 (BM).  
 Bührke, T., Brugel, E. W., and Mundt, R. 1986, *Astr. Ap.*, in press.  
 Castelaz, M. W., Grasdalén, G. L., Hackwell, J. A., Capps, R. W., and Thompson, D. 1985, *A.J.*, **90**, 1113.  
 Chandrasekhar, S., and Münch, G. 1950, *Ap. J.*, **111**, 142.  
 Cohen, M. 1983, *Rev. Mexicana Astr. Ap.*, **7**, 241.  
 Cohen, M., Biegging, J. H., and Schwartz, P. R. 1982, *Ap. J.*, **253**, 707.  
 Cohen, M., and Schmidt, G. D. 1981, *A.J.*, **86**, 1228.  
 Cohen, R. J., Rowland, P. R., and Blair, M. M. 1984, *M.N.R.A.S.*, **210**, 425.  
 Craine, E. R., Boeshaar, G. O., and Byard, P. L. 1981, *A.J.*, **86**, 751.  
 Daniel, J.-Y. 1980, *Astr. Ap.*, **87**, 204.  
 ———, 1982, *Astr. Ap.*, **111**, 58.  
 de Vegt, C. 1982, *Astr. Ap.*, **109**, L15.  
 Dolginov, A. Z., and Mytrophanov, I. G. 1978, *Astr. Ap.*, **69**, 421.  
 Draper, P. W., Warren-Smith, R. F., and Scarrott, S. M. 1985a, *M.N.R.A.S.*, **212**, 1P.  
 ———, 1985b, *M.N.R.A.S.*, **212**, 5P.  
 ———, 1985c, *M.N.R.A.S.*, **216**, 7P.  
 Dyck, H. M., Forbes, F. F., and Shawl, S. J. 1971, *A.J.*, **76**, 901.  
 Dyck, H. M., and Lonsdale, C. J. 1979, *A.J.*, **84**, 1339.  
 Elsässer, H., and Staude, H. J. 1978, *Astr. Ap.*, **70**, L3.  
 Forbes, F. F., 1971, *Ap. J. (Letters)*, **165**, L21.  
 Garrison, L. M., and Anderson, C. M. 1978, *Ap. J.*, **221**, 601.  
 Gething, M. R., Warren-Smith, R. F., Scarrott, S. M., and Bingham, R. G. 1982, *M.N.R.A.S.*, **198**, 881.  
 Hanson, R. B., Jones, B. F., and Lin, D. N. C. 1983, *Ap. J. (Letters)*, **270**, L27.  
 Hartigan, P., and Lada, C. J. 1985, *Ap. J. Suppl.*, **59**, 383.  
 Hartmann, L., and Kenyon, S. J. 1985, *Ap. J.*, **299**, 462.  
 Heckert, P. A., and Zeilik, M., II. 1981, *A.J.*, **86**, 1076.  
 ———, 1983, *M.N.R.A.S.*, **202**, 531.  
 Heckert, P. A., and Zeilik, M., II. 1984, *A.J.*, **89**, 1379.  
 ———, 1985, *A.J.*, **90**, 2291.  
 Herbig, G. H., and Rao, N. K. 1972, *Ap. J.*, **174**, 401.  
 Hodapp, K.-W. 1984, *Astr. Ap.*, **141**, 255.  
 Hough, J. H., Bailey, J., Cunningham, E. C., McCall, A., and Axon, D. J. 1981, *M.N.R.A.S.*, **195**, 429.  
 Joyce, R. R., and Simon, T. 1986, *A.J.*, **91**, 113.  
 King, D. J., Scarrott, S. M., and Taylor, K. N. R. 1983, *M.N.R.A.S.*, **202**, 1087.  
 Kobayashi, Y., Kawara, K., Maihara, T., Okuda, H., Sato, S., and Noguchi, K. 1978, *Pub. Astr. Soc. Japan*, **32**, 295.  
 Königl, A. 1982, *Ap. J.*, **261**, 115.  
 Kuhl, L. V. 1964, *Ap. J.*, **140**, 1409.  
 Lada, C. J. 1985, *Ann. Rev. Astr. Ap.*, **23**, 267.  
 Lada, C. J., and Gautier, T. N., III. 1982, *Ap. J.*, **261**, 161.  
 Lada, C. J., and Harvey, P. M. 1981, *Ap. J.*, **245**, 58.  
 Lenzen, R., Hodapp, K.-W., and Reddmann, T. 1984, *Astr. Ap.*, **137**, 365.  
 Lenzen, R., Hodapp, K.-W., and Solf, J. 1984, *Astr. Ap.*, **137**, 202.  
 McCall, A., and Hough, J. H. 1980, *Astr. Ap. Suppl.*, **42**, 141.  
 McLean, I. S., and Brown, J. C. 1978, *Astr. Ap.*, **69**, 291 (MB).  
 Ménard, F. 1986, M.Sc. thesis, Université de Montréal.  
 Ménard, F., and Bastien, P. 1987, in preparation.  
 Moneti, A., Pipher, J. L., Helfer, H. L., McMillan, R. S., and Perry, M. L. 1984, *Ap. J.*, **282**, 508.  
 Mundt, R. 1985, in *Protostars and Planets II*, ed. D. Black and M. Mathews (Tucson: University of Arizona Press), p. 414.  
 Mundt, R., Bührke, T., Fried, J. W., Neckel, T., Sarcander, M., and Stocke, J. 1984, *Astr. Ap.*, **140**, 17.  
 Mundt, R., and Fried, J. W. 1973, *Ap. J. (Letters)*, **274**, L83.  
 Mundt, R., Stocke, J., and Stockman, H. S. 1983, *Ap. J. (Letters)*, **265**, L71.  
 Mundt, R., Stocke, J., Strom, S. E., Strom, K. M., and Anderson, R., 1985, *Ap. J. (Letters)*, **297**, L41.  
 Nadeau, R., and Bastien, P. 1986, *Ap. J. (Letters)*, **307**, L5.  
 Nagata, T., Sato, S., and Kobayashi, Y. 1983, *Astr. Ap.*, **119**, L1.  
 Neckel, T., and Staude, H. J. 1984, *Astr. Ap.*, **131**, 200.  
 Nisenson, P., Stachnik, R. V., Karovska, M., and Noyes, R. 1985, *Ap. J. (Letters)*, **297**, L17.  
 Pudritz, R. E. 1985, *Ap. J.*, **293**, 216.  
 ———, 1986, in *IAU Symposium 115, Star Forming Regions*, ed. M. Peimbert and J. Jugaku (Dordrecht: Reidel), in press.  
 Pudritz, R. E., and Norman, C. A. 1983, *Ap. J.*, **274**, 677.  
 Rucinski, S. M. 1985, *A.J.*, **90**, 2321.  
 Rusk, R., and Seaquist, E. R. 1985, *A.J.*, **90**, 30.  
 Sato, S., Nagata, T., Nakajima, T., Nishida, M., Tanaka, M., and Yamashita, T. 1985, *Ap. J.*, **291**, 708.

- Scarrott, S. M., Warren-Smith, R. F., Draper, P. W., and Gledhill, T. M. 1986, *Canadian J. Phys.*, **64**, 426.
- Serkowski, K. 1969, *Ap. J.*, **156**, L55.
- Shirt, J. V., Warren-Smith, R. F., and Scarrott, S. M. 1983, *M.N.R.A.S.*, **204**, 1257.
- Simmons, J. F. L. 1982, *M.N.R.A.S.*, **200**, 91.
- Simon, T., Schwartz, P. R., Dyck, H. M., and Zuckerman, B., 1983, in *IAU Colloquium 71, Activity in Red-Dwarf Stars*, ed. P. B. Byrne and M. Rodonò (Dordrecht: Reidel).
- Snell, R. L. 1983, *Rev. Mexicana Astr. Ap.*, **7**, 79.
- Snell, R. L., Loren, R. B., and Plambeck, R. L. 1980, *Ap. J. (Letters)*, **239**, L17.
- Strom, K. M., Strom, S. E., Wolff, S. C., Morgan, J., and Wenz, M. 1986, *Ap. J. Suppl.*, **62**, 39.
- Strom, S. E. 1986, in *IAU Symposium 115, Star Forming Regions*, ed. M. Peimbert and J. Jugaku (Dordrecht: Reidel), in press.
- Taylor, K. N. R., and Storey, J. W. V. 1984, *M.N.R.A.S.*, **209**, 5P.
- Turnshek, D. A., Turnshek, D. E., and Craine, E. R. 1980, *A.J.*, **85**, 1638.
- Uchida, Y. and Shibata, K. 1984a, in *IAU Symposium 105, Unstable Current Systems and Plasma Instabilities in Astrophysics*, ed. M. Kundu and G. Holman (Dordrecht: Reidel), p. 287.
- . 1984b, *Pub. Astr. Soc. Japan*, **36**, 105.
- . 1985a, in *The Origin of Nonradiative Heating/Momentum in Hot Stars*, ed. A. B. Underhill and A. G. Michalitsianos (NASA CP-2358), p. 169.
- . 1985b, *Pub. Astr. Soc. Japan*, **37**, 515.
- Vardanian, R. A. 1964, *Soob. Bjurakan Obs.*, **35**, 3.
- Vrba, F. J., Schmidt, G. D., and Hintzen, P. M. 1979, *Ap. J.*, **227**, 185.
- Vrba, F. J., Strom, S. E., and Strom, K. M. 1976, *A.J.*, **81**, 958.
- Walsh, J. R., and Malin, D. F. 1985, *M.N.R.A.S.*, **217**, 31.
- Ward-Thomson, D., Warren-Smith, R. F., Scarrott, S. M., and Wolstencroft, R. D. 1985, *M.N.R.A.S.*, **215**, 537.
- Wolstencroft, R. D., and Simon, T. 1975, *Ap. J. (Letters)*, **199**, L165.

PIERRE BASTIEN: Département de Physique, Université de Montréal, B.P. 6128, Succ. A, Montréal, Québec, Canada H3C 3J7